Innovative Material Technology: Chaotic Motion of Single-Walled Carbon Nanotube with Linear and Nonlinear Damping

Tai-Ping Chang[1], Quey-Jen Yeh[2]
1. Department of Construction Engineering, National Kaohsiung University of Science and Technology, Kaohsiung, Taiwan
2. Department of Business Administration, National Cheng-Kung University, Tainan, Taiwan
1. E-mail: tpchang@ccms.nkfust.edu.tw
2. E-mail: yehqj@mail.ncku.edu.tw

Abstract: In the present study, the effects on chaotic behaviors of single-walled carbon nanotube (SWCNT) due to the linear and nonlinear damping are investigated. By using the Hamilton's principle, the nonlinear governing equation of the single-walled carbon nanotube embedded in a matrix is derived. The Galerkin's method is adopted to simplify the integro-partial differential equation into a nonlinear dimensionless governing equation for the SWCNT, which turns out to be a forced Duffing equation. The variations of the Lyapunov exponents of the SWCNT with damping and harmonic forcing amplitudes are investigated. Based on the computations of the top Lyapunov exponent, it is concluded that the chaotic motion of the SWCNT occurs when the amplitude of the periodic excitation exceeds certain value, besides, the chaotic motion of the SWCNT occurs with small linear damping and tiny nonlinear damping.
Keywords: chaotic motion; single-walled carbon nanotube; Lyapunov exponents; damping.

1. Introduction

Carbon nanotubes (CNTs) has drawn worldwide attention because of their potential applications in the fields of chemistry, physics, nano-engineering, electrical engineering, materials science, reinforced composite structures and construction engineering [1-3]. Recently many researches have been reported on the characteristics of vibration of nanotubes [4-8]. According to the previous theoretical and experimental studies, it is found that the mechanical behavior of nanostructures is indeed nonlinear in nature when they are subject to large external loads [9]. Among others, many researches on nonlinear vibration problems with nonlocal continuum theories have been reported [10-12]. Recently, the study of chaotic phenomena in nonlinear systems has drawn lots of attention and become a popular area of research [13-17]. However, the study about the chaotic motion of nonlinear system of single-walled carbon nanotubes is very limited, only few researches have been found in the literature [8, 18-19]. The chaotic motion is mainly attributed due to the nonlinear effects in the physical system. For a single-walled carbon nanotube (SWCNT) system, the nonlinear effects may be due to the elastic elements, nonlinear damping [20-23], system with fluids, nonlinear boundary conditions, etc. In the present study, we study the chaotic motion of nonlinear vibration of the single-walled carbon nanotube (SWCNT) subjected to linear and nonlinear damping by considering the effects of the geometric nonlinearity. The small scale effects on the nonlinear vibration of the SWCNT are considered by using the theory of nonlocal elasticity. Based on the Hamilton's principle, the nonlinear governing equations of the single-walled carbon nanotube subjected to linear and nonlinear damping are formulated. The Galerkin's method is utilized to discretize the integro-partial differential equation leading to a nonlinear dimensionless governing equation for the SWCNT, which turns out to be a forced Duffing equation with the linear and nonlinear damping. In the past, many researches have been reported on the chaotic motion of forced Duffing equations [24-27]. The main purpose of the present study is to investigate the chaotic behavior of the nonlinear dimensionless governing equation under linear and nonlinear damping by computing the Lyapunov exponents. The determination for the Lyapunov exponents has been reported in several researches [28-31].

2. Governing equation of nonlinear vibration

The single-walled carbon nanotube (SWCNT) embedded in a matrix with the linear and nonlinear damping is modeled as a single-tube pipe which has the radius R. The thickness of the tube is h, the length is L, the Young's modulus of elasticity is E and the mass density of SWCNT is ρ. The linear damping coefficient of the matrix is c_1 and the nonlinear damping coefficient of the matrix is c_3. In addition, the boundary conditions of the SWCNT

are considered as simply-supported at both ends. Based on the Hamilton's principle and nonlocal elasticity theory, the nonlocal governing equations of the SWCNT in terms of the displacements can be obtained as follows:

$$EI\frac{\partial^4 w}{\partial x^4}+\left[\frac{\mathrm{EA}}{2L}\int_0^L\left(\frac{\partial w}{\partial x}\right)^2 dx\right]\frac{\partial^2}{\partial x^2}\left[\left(e_0a\right)^2\frac{\partial^2 w}{\partial x^2}-w\right]=\rho\mathrm{A}\frac{\partial^2}{\partial \bar{t}^2}\left[\left(e_0a\right)^2\frac{\partial^2 w}{\partial x^2}-w\right]$$
$$+c_1\frac{\partial}{\partial \bar{t}}\left[\left(e_0a\right)^2\frac{\partial^2 w}{\partial x^2}-w\right]+c_3\frac{\partial}{\partial \bar{t}}\left[\left(e_0a\right)^2\frac{\partial^2 w}{\partial x^2}-w\right]^3+q(x,\bar{t})-\left(e_0a\right)^2\frac{\partial^2 q(x,\bar{t})}{\partial x^2} \quad (1)$$

where $\bar{t}$ denotes the time, $q(x,\bar{t})$ is distributed transverse load, e_0 is a constant appropriate to each material, a is an internal characteristic length (e.g., length of C–C bond, lattice parameter, and granular distance). Beside, $c_1$and c_3 are the linear and nonlinear damping coefficients respectively. In this study, we consider the nonlinear viscous damping since it is shown more effective in suppressing the resonant peak of a nonlinear system than linear damping, furthermore, the damping in SWCNT system is found to strongly depend on the amplitude of motion, and can be described by a nonlinear rather than a linear damping force [20-23]. Now we utilize one term approximation to obtain the displacement for the nonlinear system based on Galerkin's approach, then the displacement function can be written as follows:

$$w(x,\bar{t})=\bar{W}(\bar{t})\sin\frac{\pi x}{L} \quad (2)$$

where $\bar{W}(\bar{t})$ is the function of time $\bar{t}$.

Substituting Eq. (2) into Eq. (1), multiplying $\sin(\pi x/L)$ and integrating along the nanotube length, we can come up with the following nonlinear differential equation:

$$\frac{d^2\bar{W}}{d\bar{t}^2}+\omega_0^2\bar{W}+C_1\frac{d\bar{W}}{d\bar{t}}+K_N\bar{W}^3+C_3\left(\frac{d\bar{W}}{d\bar{t}}\right)^3=\bar{Q}_0+\bar{Q}_1(\bar{t}) \quad (3)$$

where

$$\omega_0=\sqrt{\frac{1}{\rho\mathrm{A}}\left[\frac{\mathrm{EI}(\pi/L)^4}{1+\left(e_0a\right)^2(\pi/L)^2}\right]},C_1=\frac{c_1}{\rho\mathrm{A}},K_N=\frac{\mathrm{E}\pi^4}{4\rho L^4},C_3=\frac{3c_3}{4\rho\mathrm{A}}. \quad (4)$$

In addition, $\bar{Q}_0$ denotes the time-independent loading and $\bar{Q}_1(\bar{t})$ denotes the time-dependent loading individually. For convenience, the following parameters are introduced to deal with the tiny values in nano systems:

$$W=\frac{\bar{W}}{L},t=\frac{\bar{t}}{T},T=\sqrt{\rho A\left[\frac{1+\left(e_0a\right)^2(\pi/L)^2}{\mathrm{EI}(\pi/L)^4}\right]} \quad (5)$$

Substituting Eq. (5) into Eq. (3), the following dimensionless equations are obtained:

$$\frac{d^2W}{dt^2}+W+\mu_1\frac{dW}{dt}+\gamma W^3+\mu_3\left(\frac{dW}{dt}\right)^3=Q_0+Q_1\cos(\Omega t) \quad (6)$$

where

$$\mu_1=C_1T,\ \gamma=K_NT^2L^2,\ \mu_3=C_3\frac{L^2}{T},$$
$$Q_0=\bar{Q}_0\frac{T^2}{L},\ Q_1\cos(\Omega\mathrm{t})=\bar{Q}_1(\bar{t})\frac{T^2}{L}. \quad (7)$$

where the time-dependent loading is assumed as a periodic excitation, and Ω is the driving frequency of the periodic loading. Eq. (6) is a forced Duffing equation with the linear and nonlinear damping.

3. Chaotic motion of nonlinear system

The main purpose of the present study is to investigate the chaotic motion of the nonlinear differential equation shown in Eq. (6) by evaluating Lyapunov exponents. The chaotic phenomena occurs when the top Lyapunov exponent changes from negative to positive. In order to compute Lyapunov exponents, it is necessary to study the growth of vectors tangent to the surface defined by the equations of motion in the phase space of the

physical system. In the present study, the approach to evaluate Lyapunov exponents is based on Wolf's algorithm [28] and numerical methods in Refs. [29,30] so that the system as defined in Eq. (6) can be written into the following simultaneous equations, with

$$W = W_1,\ \dot{W} = W_2,\ t = W_3:$$

$$\dot{W}_1 = W_2 \tag{8}$$

$$\dot{W}_2 = -W_1 - \gamma W_1^3 - \mu_1 W_2 - \mu_3 W_2^3 + Q_0 + Q_1 \cos(\Omega t) \tag{9}$$

$$\dot{W}_3 = 1.0 \tag{10}$$

where " • " denotes $\frac{d}{dt}$.

Based on Wolf's basic idea, is it necessary to evaluate the long-term evolution of an infinitesimal n-sphere, here n=3, of initial conditions. Lyapunov exponents are denoted as follows:

$$\lambda_i = \lim_{t\to\infty} \frac{1}{t} \log_2 \frac{d_i(t)}{d_i(0)} \quad i = 1,2,3 \tag{11}$$

where λ_i are ordered from largest to smallest and $d_i(t)$ are the lengths of the ellipsoidal principal axes of the sphere. In order to be consistent with the definition of Lyapunov exponents, the separations of the initial conditions must be as small as the computer limitations tolerance. The nonlinear differential equations are integrated with these different initial conditions. However, in a chaotic system, the conditions of small separations can't be guaranteed, which is required for the convergence of Lyapunov exponents spectrums. In order to cope with this problem, a "reference" trajectory is set up by the action of the nonlinear equations on some initial conditions. Then the trajectories of points on the surface of the sphere are computed by integrating the linearized equations of motion utilizing initial conditions infinitesimally separated from the reference trajectory. The principal axes are denoted by the evolution from the linearized equations of an initially orthonormal vector frame fixed to the reference trajectory. For a system shown in Eq. (6), dimension n=3 and nine linearized equations can be established. In Eq. (8-10), there are several parameters which can influence the chaotic motion of the system, such as γ, μ_1, μ_3, Q_0, Q_1, Ω and the initial conditions.

4. Effects on chaotic motion due to linear and nonlinear damping

First of all, we deal with the system without the effects of nonlinear damping parameter μ_3 and fix all the parameters except Q_1, we vary the amplitude of the periodic excitation from Q_1=0 to a certain value when the top Lyapunov exponents change from negative to positive, that is when the chaotic motion occurs. After that we increase the value of Q_1 gradually, then at certain value of Q_1, the top Lyapunov exponents will change from positive to negative which implies that the motion of the system will change from chaotic motion to periodic motion until we hit the next critical value when the top Lyapunov exponents will change from negative to positive. The main purpose of the present study is to investigate the chaotic motion of the system shown in Eq. (6) with linear damping and nonlinear damping based on the computation of the top Lyapunov exponents, Therefore, after the first critical value of Q_1 is found, we fix the value of Q_1 slightly bigger than the critical one and all the parameters except the linear damping parameter μ_1. Then we can study the effect of linear damping parameter on the chaotic motion of the system based on the computation of the top Lyapunov exponents. As we increase the value of linear damping parameter gradually, the top Lyapunov exponents will change from positive to negative at a certain value of $\mu_1$so that the system will change from chaotic to periodic motion. Finally we fix all the parameters except the nonlinear damping parameter to study the effect of nonlinear damping parameter on the chaotic motion of the system, it can be detected that with a small value of nonlinear damping parameter, the top Lyapunov exponents of the system would change from positive to negative so that the chaotic motion of the system would switch back to periodic motion.

5. Numerical examples and discussions

In the numerical computations, the simply supported boundary conditions are considered for the SWCNT. The dimensionless governing equation for SWCNT is written as in Eq (6), the main purpose of the present study is to investigate the chaotic motion for the nonlinear system in Eq. (6) with linear and nonlinear damping; therefore, the investigations are divided into two sections below.

5.1 Nonlinear system with linear damping only, μ_3=0.

First of all, the numerical values of the parameters in Eq. (6) are fixed as follows:

$$\mu_1 = 0.1,\ \gamma = 1.0,\ \mu_3 = 0.0,\ Q_0 = 3.0,\ \Omega = 1.0. \tag{12}$$

In addition, the initial conditions in Eqs. (8-10) are as follows:

$$W_1(0)=1.0,\ W_2(0)=0.0,\ W_3(0)=0.0 \tag{13}$$

Now we gradually vary the amplitude of the periodic excitation Q_1 from Q_1=0 to Q_1=30.0. As we can see from Figs. 1a-1d, Lyapunov exponents of the system are computed for different values of Q_1. In Figs. 1a-1b, the top Lyapunov exponent is computed as λ_1= -0.00022 when Q_1=14.31 as shown in Fig 1a; while λ_1= +0.00178 when Q_1=14.32 as shown in Fig. 1b. Therefore, the system is originally stable under Q_1=14.31 because the top Lyapunov exponent is negative, then appears to be losing its stability when Q_1=14.32 because the top Lyapunov exponent changes from negative into positive, which implies the chaotic motion occurs when Q_1 is slightly larger than 14.32. Furthermore, we gradually vary the amplitude of the periodic excitation from Q_1=14.32 to Q_1=30.0, as we can see from Figs. 1c-1d, the top Lyapunov exponent is computed as λ_1= -0.00107 when Q_1=23.72, then turns into λ_1= +0.00046 when Q_1=23.73. Therefore, we conclude that the first critical value to produce the chaotic motion for the system is Q_1=14.32, while the second critical value is Q_1=23.73. Now we fix the value of Q_1 as Q_1=16.0, which is slightly bigger than the first critical value 14.32, all the other parameters remain the same as those in Eqs. (12-13). In Figs. 2a-2c, we plot the time history, phase portrait and Poincare map of SWCNT. As we can detect from Fig. 2c, the chaotic motion of the system is quite obvious. It is well known that the displacement of the system gets smaller as the linear damping parameter increases. In Figs. 3a-3f, we evaluate the Lyapunov exponents by increasing the linear damping parameter from μ_1=0.1 to μ_1=0.8 individually. As we can detect from Figs. 3a-3b, the top Lyapunov exponents are still positive up to μ_1=0.28, however, when μ_1=0.29 the top Lyapunov exponent becomes negative as shown in Fig. 3c, furthermore, if we increase the linear damping parameter from μ_1=0.3 to μ_1=0.8, the top Lyapunov exponents remain positive all the way which is fairly reasonable. In Figs. 4a-4c, we present the corresponding Poincare maps for different values of linear damping parameter μ_1=0.3,0.5,0.8 individually, it is quite understood to notice that all the Poincare maps show periodic motion for the nonlinear system. On the other hand, if we decrease the linear damping parameter from μ_1=0.1 down to μ_1=0.01,0.005, the top Lyapunov exponents are positive as shown in Figs.5a-5b, which implies that the chaotic motion occurs for the nonlinear system. Figs 6a-6b present the corresponding Poincare maps for different values of nonlinear damping parameter μ_1=0.01,0.005 separately. Based on the above numerical computations, the chaotic motion will occur with small linear damping until the linear damping parameter exceeds the critical linear damping value, in the present case, μ_1=0.29.

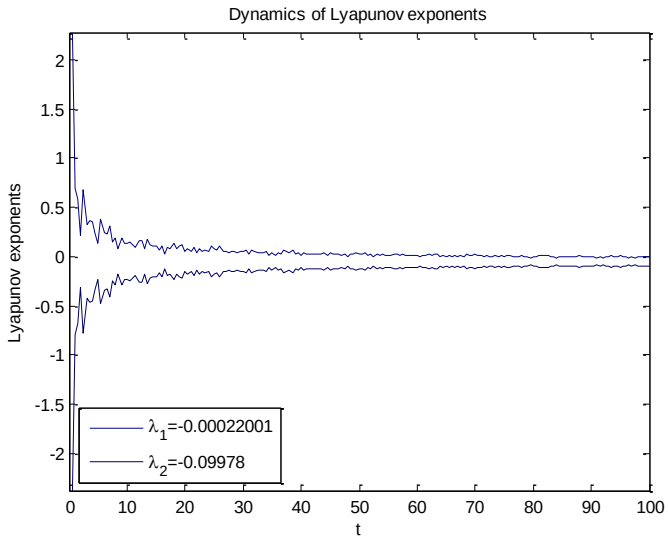

Fig. 1a. Lyapunov exponents versus time for Q_1=14.31.

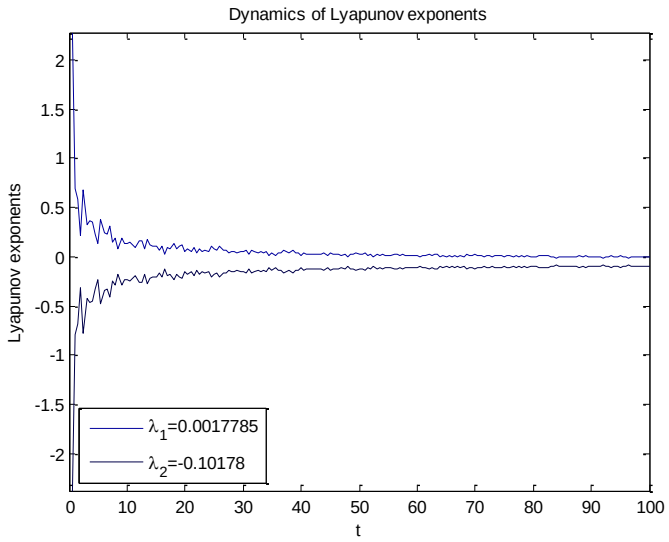

Fig. 1b. Lyapunov exponents versus time for Q_1=14.32.

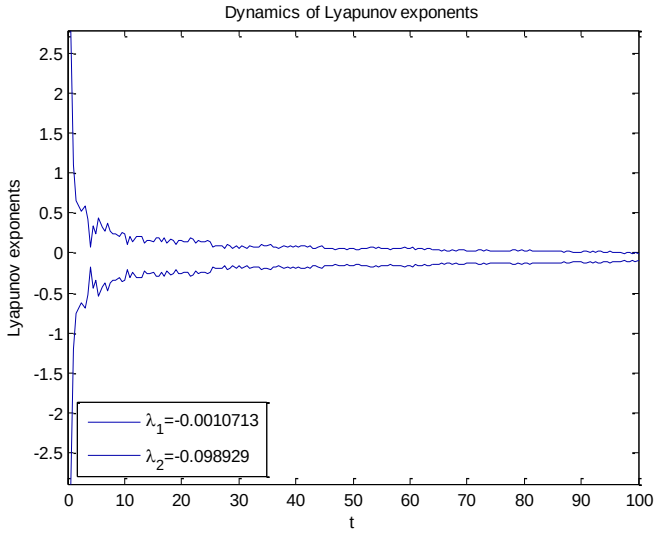

Fig. 1c. Lyapunov exponents versus time for Q_1=23.72.

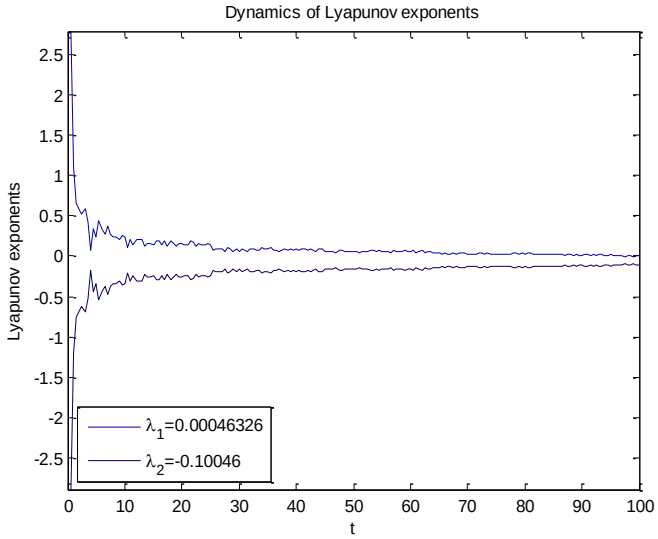

Fig. 1d. Lyapunov exponents versus time for Q_1=23.73.

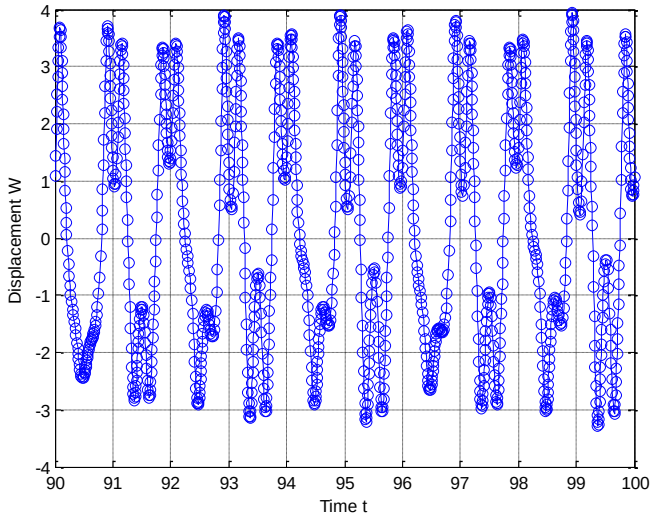

Fig. 2a. Time history of SWCNT. (μ_1=0.1, γ=1.0, μ_3=0.0, Q_0=3.0, Ω=1.0, Q_1=16.0)

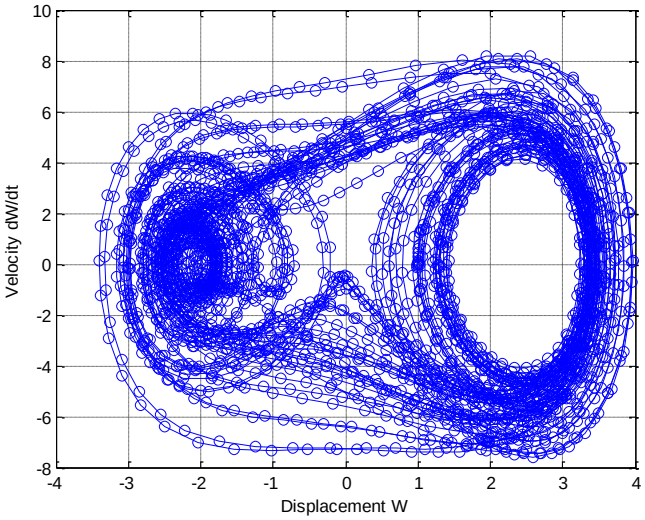

Fig. 2b. Phase portrait of SWCNT. (μ_1=0.1, γ=1.0, μ_3=0.0, Q_0=3.0, Ω=1.0, Q_1=16.0)

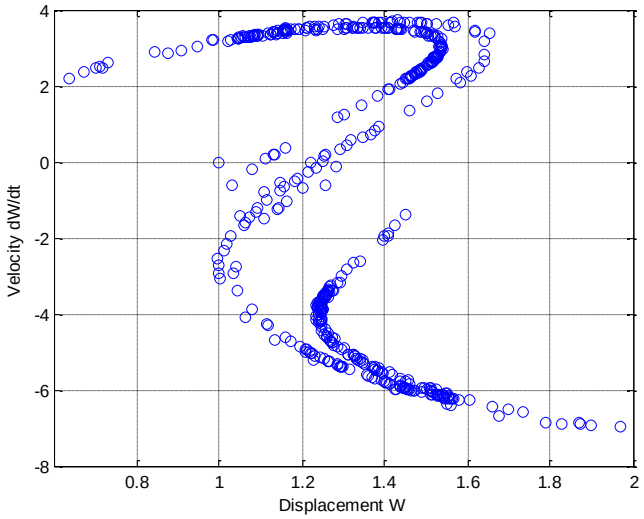

Fig. 2c. Poincare map of SWCNT. (μ_1=0.1, γ=1.0, μ_3=0.0, Q_0=3.0, Ω=1.0, Q_1=16.0)

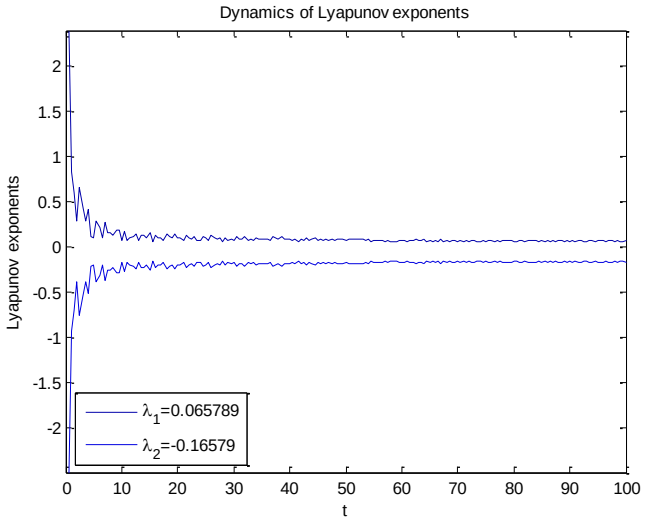

Fig. 3a. Lyapunov exponents versus time for μ_1=0.1.

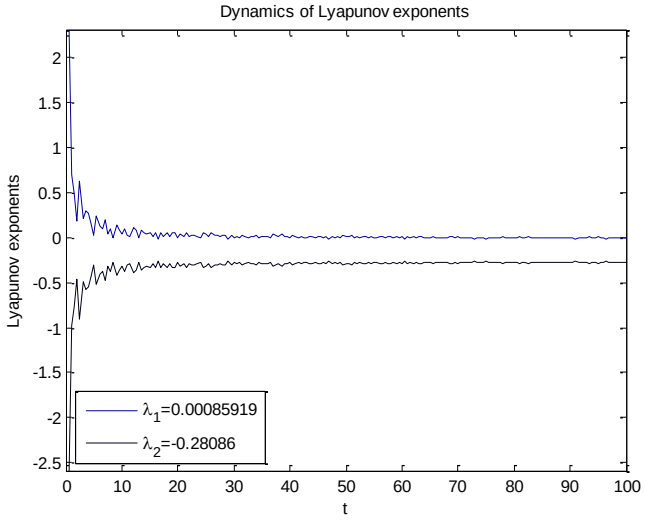

Fig. 3b. Lyapunov exponents versus time for μ_1=0.28.

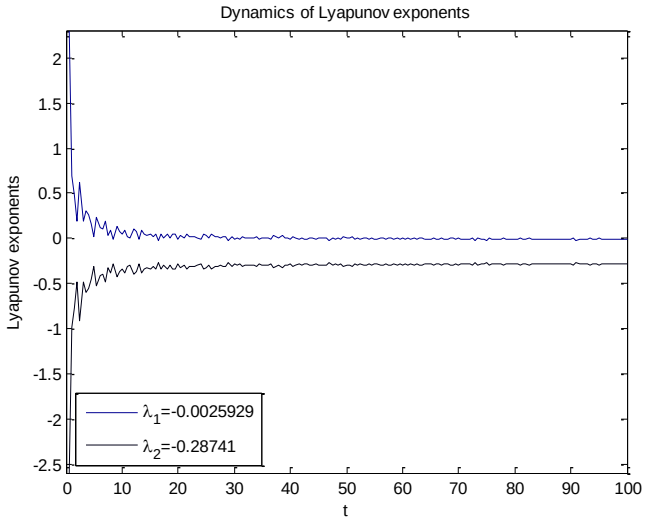

Fig. 3c. Lyapunov exponents versus time for μ_1=0.29.

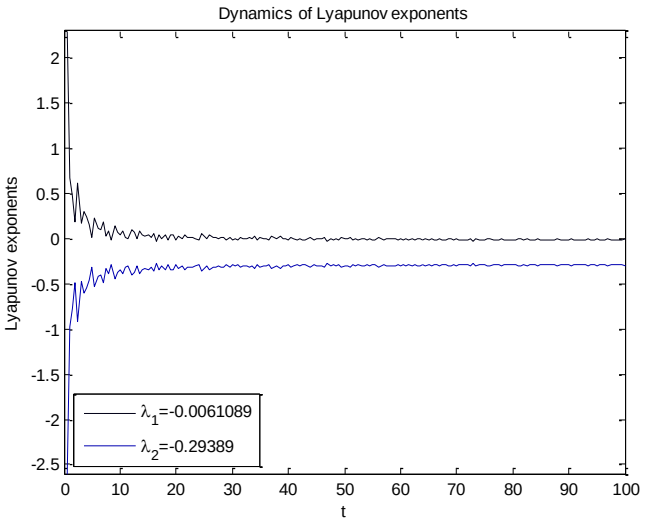

Fig. 3d. Lyapunov exponents versus time for μ_1=0.30.

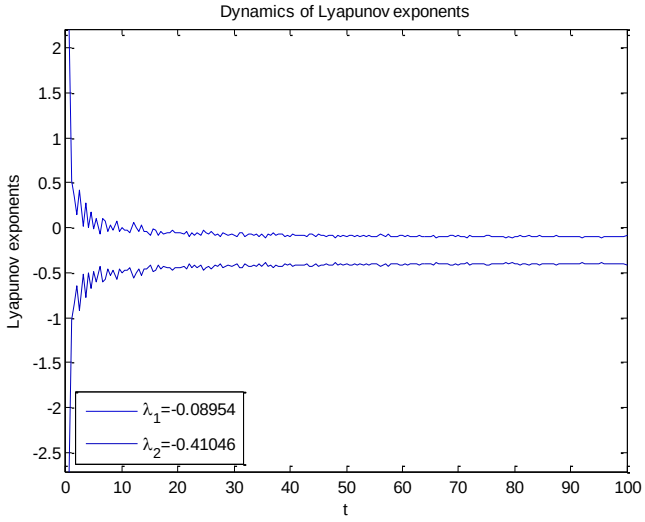

Fig. 3e. Lyapunov exponents versus time for μ_1=0.5.

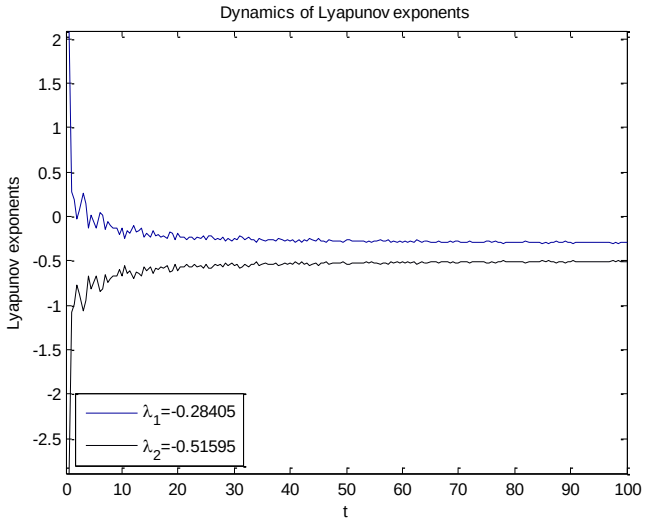

Fig. 3f. Lyapunov exponents versus time for μ_1=0.8.

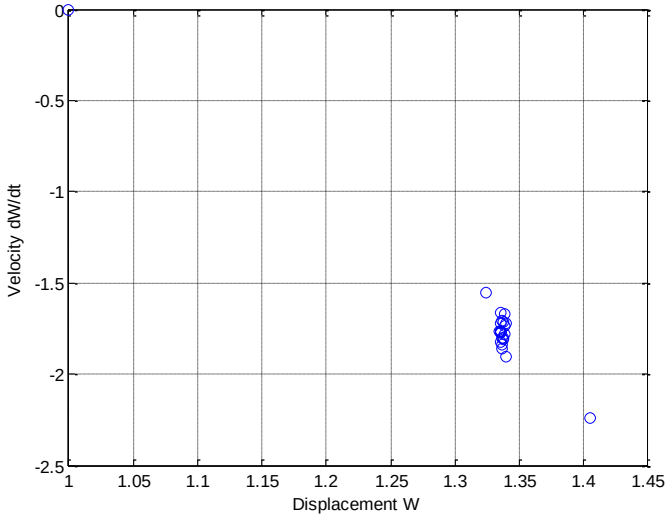

Fig. 4a. Poincare map of SWCNT. (μ_1=0.3, γ=1.0, μ_3=0.0, Q_0=3.0, Ω=1.0, Q_1=16.0)

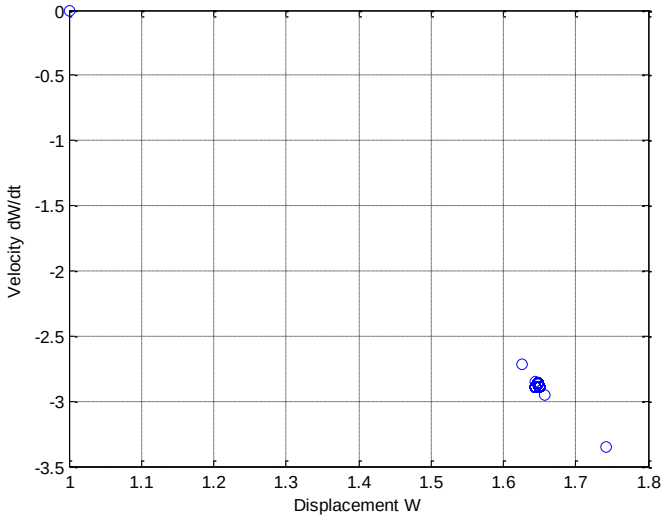

Fig. 4b. Poincare map of SWCNT. (μ_1=0.5, γ=1.0, μ_3=0.0, Q_0=3.0, Ω=1.0, Q_1=16.0)

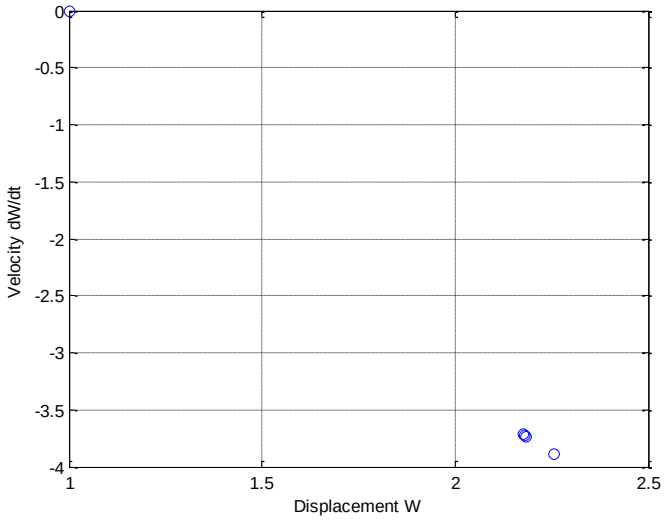

Fig. 4c. Poincare map of SWCNT. (μ_1=0.8, γ=1.0, μ_3=0.0, Q_0=3.0, Ω=1.0, Q_1=16.0)

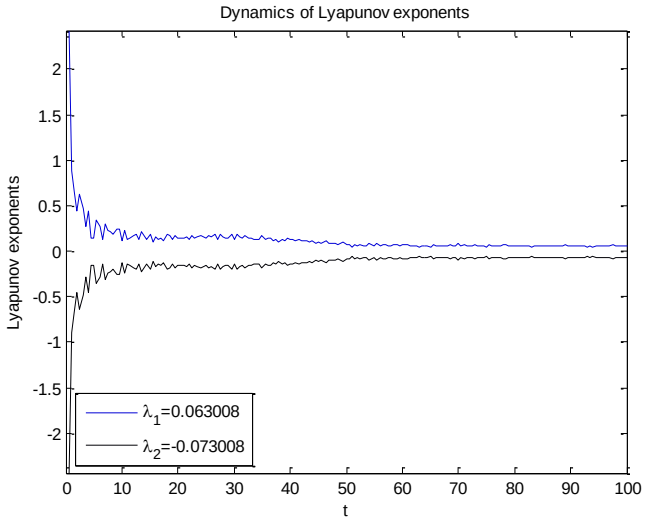

Fig. 5a. Lyapunov exponents versus time for μ_1=0.01.

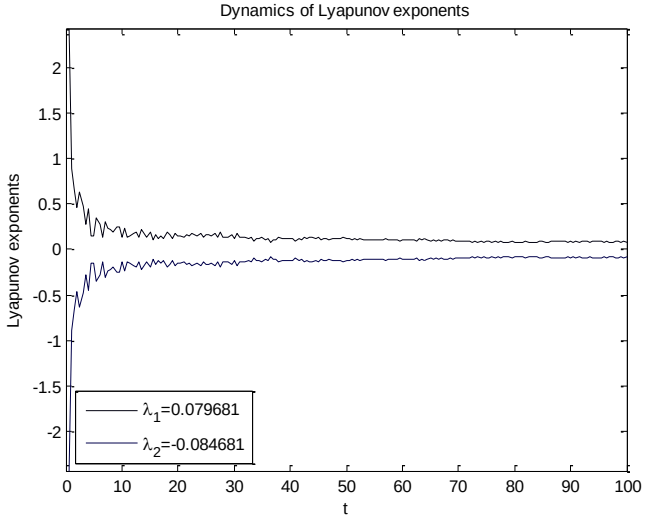

Fig. 5b. Lyapunov exponents versus time for μ_1=0.005.

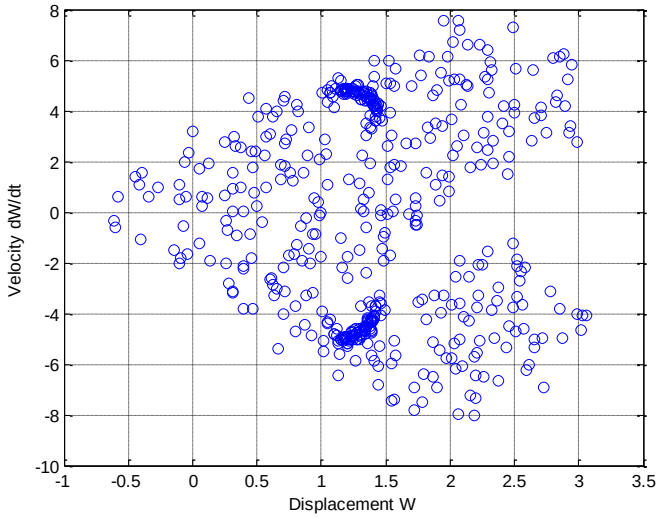

Fig. 6a. Poincare map of SWCNT. (μ_1=0.01, γ=1.0, μ_3=0.0, Q_0=3.0, Ω=1.0, Q_1=16.0)

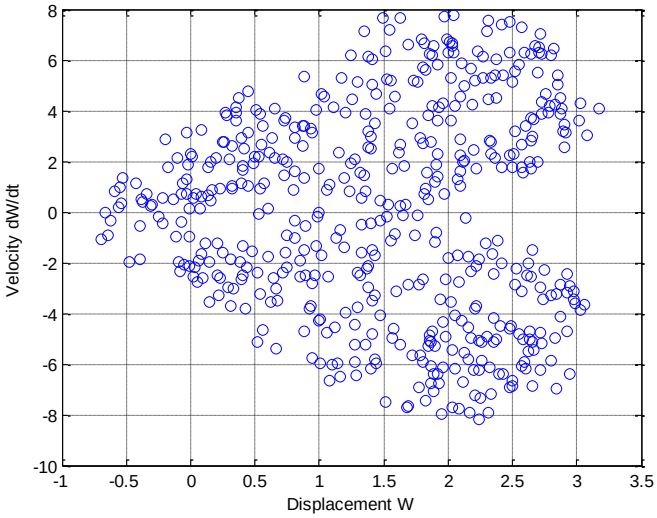

Fig. 6b. Poincare map of SWCNT. (μ_1=0.005, γ=1.0, μ_3=0.0, Q_0=3.0, Ω=1.0, Q_1=16.0)

5.2 Nonlinear system with linear damping and nonlinear damping

Now we are ready to study the chaotic motion of the nonlinear system with both the linear and nonlinear damping. Here we adopt the same data as those in Eqs. (12-13) except the nonlinear damping parameter is added. Besides, we fix the amplitude of the periodic excitation as Q_1=16.0 because it is slightly over the first critical value to create the chaotic motion for the nonlinear system. We gradually increase the value of nonlinear damping from μ_3=0.001 to μ_3=0.1 for the system, the Lyapunov exponents are shown in Figs. 7a-7e for different value of nonlinear damping. It can be seen from Fig. 7b that the top Lyapunov exponent is λ_1= +0.0041421when μ_3=0.0055; while the top Lyapunov exponent is λ_1= -0.00047663 when μ_3=0.0060 as shown in Fig. 7c. Then the top Lyapunov exponent remains negative from μ_3=0.0060 to μ_3=0.10 as shown in Figs. 7c-7e. Therefore, we can conclude that the chaotic motion of the system still happens with tiny nonlinear damping until μ_3=0.0060, when the nonlinear damping parameter is larger than 0.006, the periodic motion of the system is expected to appear. The corresponding Poincare maps are presented in Figs. 8a-8c, as it can be detected from Fig 8a, the nonlinear system still presents chaotic phenomena

with tiny nonlinear damping parameter, however, the nonlinear system regains its stability, namely, periodic motion, with nonlinear damping parameter bigger than 0.006 as seen from Figs. 8b-8c. Based on the above numerical computations, the chaotic motion will occur with tiny nonlinear damping until the nonlinear damping parameter exceeds the critical damping value, in the present case, μ_3=0.0060.

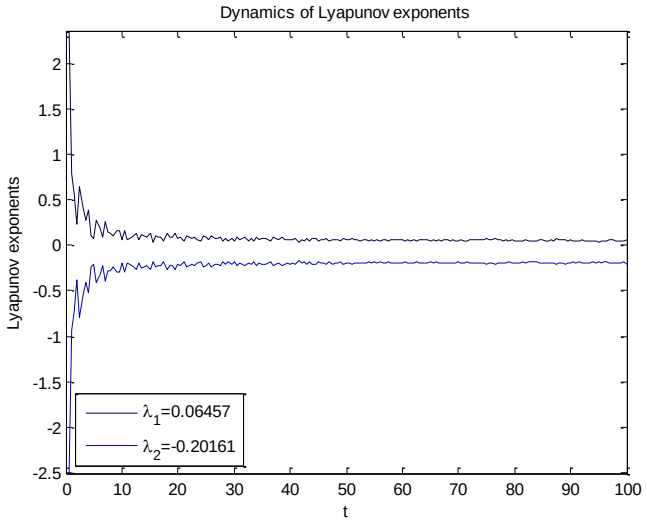

Fig. 7a. Lyapunov exponents versus time for μ_1=0.1, μ_3=0.001.

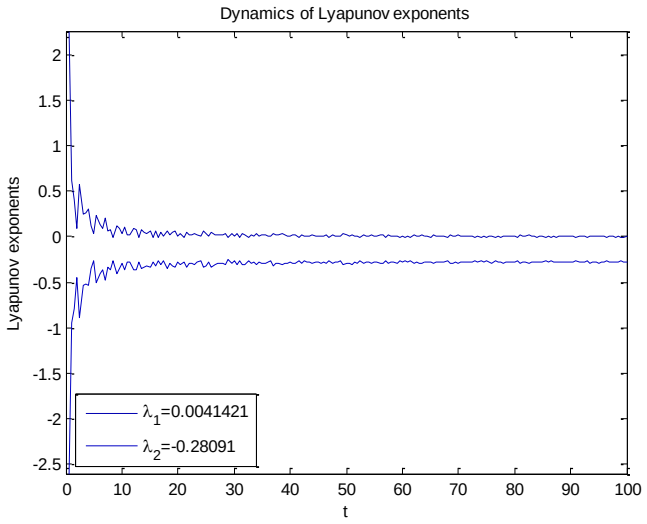

Fig. 7b. Lyapunov exponents versus time for μ_1=0.1, μ_3=0.0055.

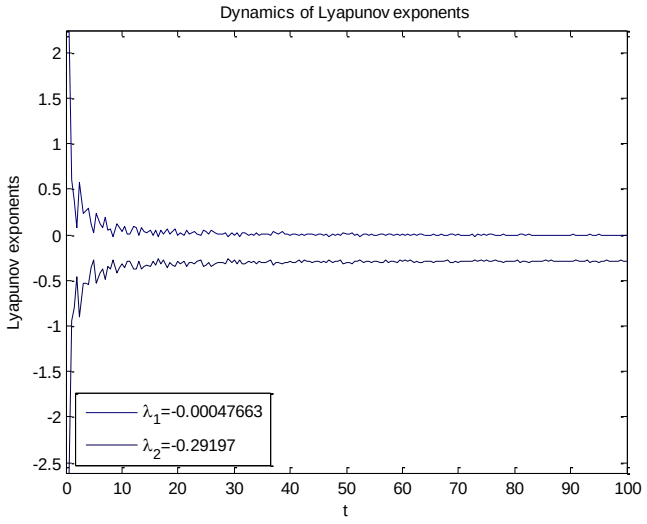

Fig. 7c. Lyapunov exponents versus time for μ_1=0.1, μ_3=0.006.

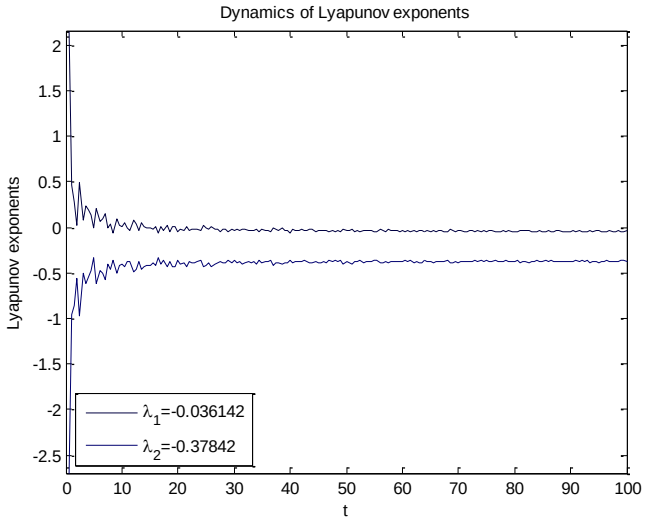

Fig. 7d. Lyapunov exponents versus time for μ_1=0.1, μ_3=0.001.

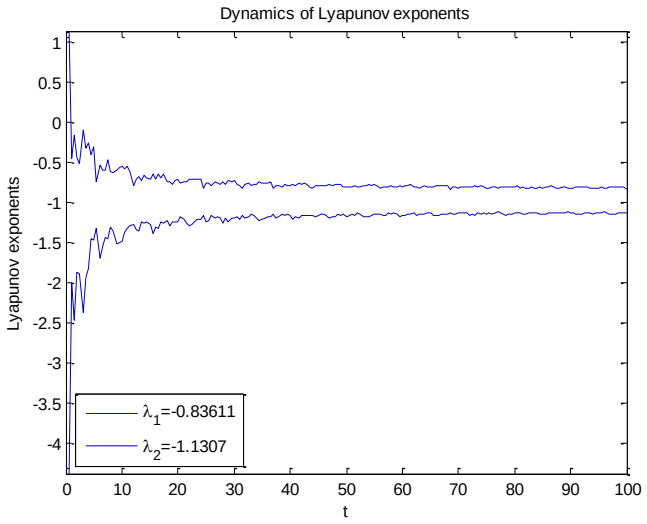

Fig. 7e. Lyapunov exponents versus time for μ_1=0.1, μ_3=0.1.

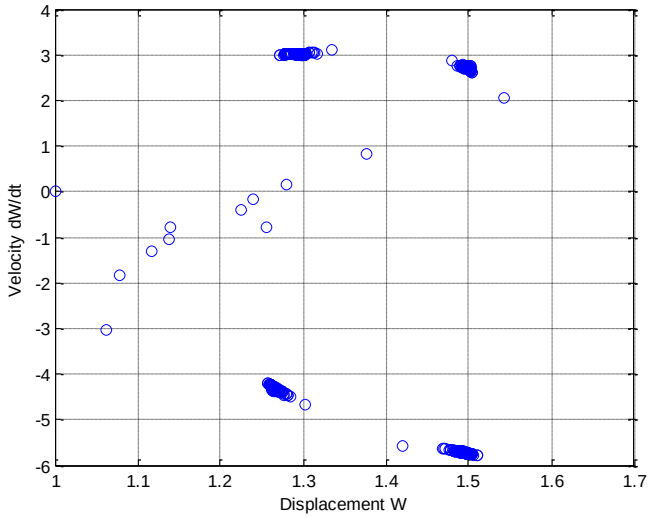

Fig. 8a. Poincare map of SWCNT. (μ_1=0.1, γ=1.0, μ_3=0.001, Q_0=3.0, Ω=1.0, Q_1=16.0)

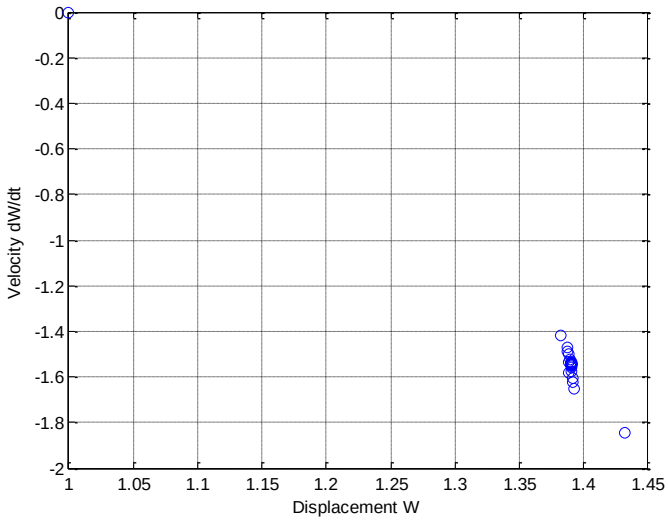

Fig. 8b. Poincare map of SWCNT. (μ_1=0.1, γ=1.0, μ_3=0.01, Q_0=3.0, Ω=1.0, Q_1=16.0)

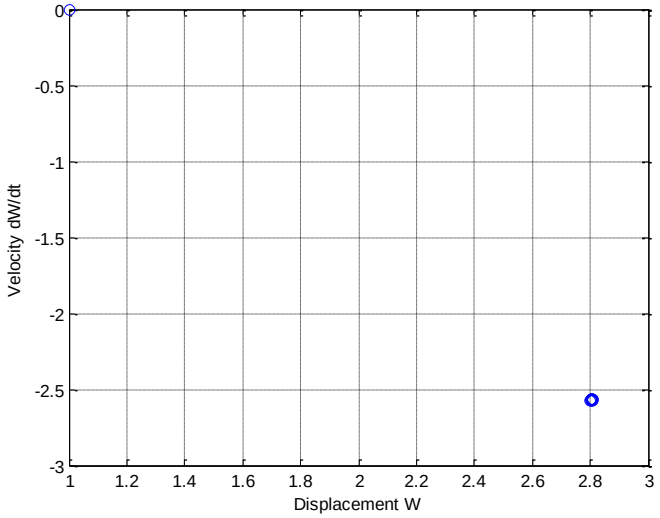

Fig. 8c. Poincare map of SWCNT. (μ_1=0.1, γ=1.0, μ_3=0.1, Q_0=3.0, Ω=1.0, Q_1=16.0)

5. Conclusions

In the present study, we investigate the effects on chaotic behaviors of single-walled carbon nanotube (SWCNT) due to the linear and nonlinear damping. By using the Hamilton's principle, the nonlinear governing equation of the single-walled carbon nanotube embedded in a matrix is derived. We utilize the Galerkin's method to discretize the integro-partial differential equation leading to a nonlinear dimensionless governing equation for the SWCNT, which turns out to be a forced Duffing equation with the linear and nonlinear damping. The chaotic phenomena occurs when the top Lyapunov exponent of the forced Duffing equation changes from negative to positive. Based on the computations of the top Lyapunov exponent, we can conclude that the chaotic motion of the nonlinear system occurs when the amplitude of the periodic excitation exceeds certain value by fixing all the other parameters. When the nonlinear system is without the nonlinear damping, the chaotic motion occurs with small linear damping until the linear damping parameter exceeds the critical linear damping value. Furthermore, if the system is with both the linear and nonlinear damping, the chaotic motion occurs with tiny nonlinear damping until the nonlinear damping parameter exceeds the critical damping value.

Acknowledgements

This research was partially supported by the Ministry of Science and Technology in Taiwan through Grant No. MOST-103-2221-E-327-011. The authors are grateful for the financial support.

References

[1] Iijima S. Helical microtubules of graphitic carbon. Nature 1991;354:56–8.
[2] Lau KT, Gu C, Hui D. A critical review on nanotube and nanotube/nanoclay related polymer composite materials. Compos. Part B 2006;37:425–36.
[3] Spitalsky Z, Tasis D, Papagelis K, Galiotis C. Carbon nanotube-polymer composites: chemistry, processing, mechanical and electrical properties. Prog Polym Sci 2010;35:357–401.
[4] Xia W, Wang L. Vibration characteristics of fluid-conveying carbon nanotubes with curved longitudinal shape, Comput Mater Sci 2010;49:99–103.
[5] Ghavanloo E, Rafiei M, Daneshmand F. In-plane vibration analysis of curved carbon nanotubes conveying fluid embedded in viscoelastic medium. Phys Lett A 2011:375:1994–9.
[6] Simsek M. Vibration analysis of a single-walled carbon nanotube under action of a moving harmonic load based on nonlocal elasticity theory. Phys E 2010;43: 182–91.
[7] Chang TP. Thermal–mechanical vibration and instability of a fluid-conveying single-walled carbon nanotube embedded in an elastic medium based on nonlocal elasticity theory. Appl Math Modell 2012;36:1964–73.
[8] Hawwa MA, Al-Qahtani HM. Nonlinear oscillations of a double-walled carbon nanotube. Comput Mater Sci 2010;48:140-3.

[9] Yang J, Ke LL, Kitipornchai S. Nonlinear free vibration of single-walled carbon nanotubes using nonlocal Timoshenko beam theory. Physica E 2010;42:1727–35.
[10] Fang B, Zhen YX, Zhang CP, Tang Y. Nonlinear vibration analysis of double-walled carbon nanotubes based on nonlocal elasticity theory. Appl Math Modell 2013;37:1096–107.
[11] Chang TP. Nonlinear thermal-mechanical vibration of flow-conveying double-walled carbon nanotubes subjected to random material property. Microfluid Nanofluid 2013;15:219-29.
[12] Simsek M. Large amplitude free vibration of nanobeams with various boundary conditions based on the nonlocal elasticity theory. Compos. Part B 2014;56:621-8.
[13] Yu YY. Equations for large deflections of homogeneous and layered beams with application to chaos and acoustic radiation. Compos Engr 1992;2:117-136.
[14] Hohe J, Librescu L. Recent results on the effect of the transverse core compressibility on the static and dynamic response of sandwich structures. Compos. Part B 2008;39:108-119.
[15] Hao YX, Zhang W, Yang J. Nonlinear oscillation of a cantilever FGM rectangular plate based on third-order plate theory and asymptotic perturbation method. Compos. Part B 2011;42:402-413.
[16] Ansari R, Mohammadi V, Faghih Shojaei M, Gholami R, Sahmani S. On the forced vibration analysis of Timoshenko nanobeams based on the surface stress elasticity theory. Compos. Part B 2014;60:158-166.
[17] Rezaee M, Jahangiri R. Nonlinear and chaotic vibration and stability analysis of an aero-elastic piezoelectric FG plate under parametric and primary excitations. Sound Vib 2015;344:277-296.
[18] Mayoof FN, Hawwa MA. Chaotic behavior of a curved carbon nanotube under harmonic excitation. Chaos Solitons Fractals 2009;42:1860-1867.
[19] Kim IK, Lee SI. Nonlinear responses of a single-wall carbon nanotube cantilever. Physica E 2015;67:159-167.
[20] Eichler A, et al. Nonlinear damping in mechanical resonators made from carbon nanotubes and graphene. Nature Nanotechnology 2011;6:339-342.
[21] Sazonova V, et al. Tunable carbon nanotube electromechanical oscillator. Nature 2004;431:284–287.
[22] Steele GA, et al. Strong coupling between single-electron tunneling and nanomechanical motion. Science 2009;325:1103–1107.
[23] Lassagne B, Tarakanov Y, Kinaret J, Garcia-Sanchez D, Bachtold A. Coupling mechanics to charge transport in carbon nanotube mechanical resonators. Science 2009;325:1107–1110.
[24] Dooren RV, Janssen H. A continuation algorithm for discovering new chaotic motions in forced Duffing systems. J Comput Appl Math 1996;66:527-41.
[25] Han X, Bi Q. Bursting oscillations in Duffing's equation with slowly changing external forcing. Commu Nonlinear Sci Numer Simulat 2011;16:4146-52.
[26] Akhmet MU, Fen MO. Chaotic period-doubling and OGY control for the forced Duffing equation. Commu Nonlinear Sci Numer Simulat 2012;17:1929-46.
[27] Sharma A, Patidar V, Purohit G, Sud KK. Effects on the bifurcation and chaos in forced Duffing oscillator due to nonlinear damping. Commu Nonlinear Sci Numer Simulat 2012;17:2254-69.
[28] Wolf A, Swift JB, Swinney HL, Vastano JA. Determining Lyapunov exponents from a time series. Physica D 1985;16:285-317.
[29] Zeni AR, Gallas JAC. Lyapunov exponents for a Duffing oscillator. Physica D, 1995;89:71-82.
[30] Wei JG, Leng G. Lyapunov exponent and chaos of Duffing's equation perturbed by white noise. Appl Math Comput 1997;88:77-93.
[31] Wu GC, Baleanu D. Jacobian matrix algorithm for Lyapunov exponents of the discrete fractional maps. Commu Nonlinear Sci Numer Simulat 2015;22:95-100.